JOURNAL OF MATERIALS SCIENCE 32 (1997) 6475–6481

Influence of solids loading on the green microstructure and sintering behaviour of ceramic injection mouldings

DEAN-MO LIU, WENJEA J. TSENG
Materials Research Laboratories, Industrial Technology Research Institute, Chutung, Hsinchu 31015 Taiwan

The influence of solid loading of ceramic injection mouldings containing 45–60 vol % submicrometre zirconia powders on the green microstructure and sintering behaviour was investigated. The mouldings with lower solids content exhibit a coarser green microstructure, which, in turn, shows lower sintering activity. The sintering activity is largely improved by increasing the solids loading to 60% at which a sintered density of 99% theoretical can easily be attained at 1400 °C, which is primarily because of the evolution of a finer green microstructure. The green microstructure of the mouldings, along with the sintering behaviour, was found to be well correlated with the average pore diameter, rather than the most-frequent pore diameter in the pore-size frequency distribution of the green compacts. The moulded compacts, although containing considerable amount of agglomerates, show isotropic shrinkage behaviour.

1. Introduction

In ceramic powder processing, the injection moulding technique has been receiving great attention for many years [1–3] primarily because of its attractive ability for mass production of ceramic parts with complex shape and with relatively high dimensional precision. Among a vast number of investigations, the removal of organic binder from injection mouldings has been the most investigated object of many publications [4–6]. However, little study in the area of injection moulding has been addressed to the relationship between green microstructure after binder removal and subsequent sintering behaviour and this is probably because green-to-sinter property has already been an interesting subject for some years [7–10].

It has been demonstrated by the present authors that the binder in the wax-based zirconia mouldings currently fabricated can be thermally removed (i.e. thermolysis) at a reasonable heating rate without generating defects such as large internal voids, bloating, and surface cracking [11]. This encourages us to investigate further how green microstructure will be developed within the mouldings of differing starting solid contents and how the resulting green microstructure affects sintering behaviour. The latter subject has received much attention over the past decade; however, it is limited to powder consolidation techniques other than injection moulding. In fact, without considering consolidation techniques, a given powder assembly frequently results in a specific sintered microstructure at a specific sintering cycle.

Since the sintering behaviour involves both densification and grain growth events, the particle packing efficiency or, correspondingly, the pore-size distribution within the green powder compacts acquires an increasingly important role in dominating sinterability. Many attempts have been focused on correlating green properties such as particle-size or pore-size distribution of the powder compact with densification [8, 10, 12–15]. Among them, the importance of pore-size distribution has been particularly stressed, primarily because the densification is essentially a process for pore elimination. Many investigations revealed that homogeneous pore-size distribution is principally responsible for enabling the powder compacts to reach a high end-point density. Recently, Roosen and Bowen [10] attempted to correlate the sintering behaviour with green property of the powder compacts made from a variety of consolidation techniques. They suggested that the maximum pore diameter in the pore-size distribution (they termed it the *most frequent pore diameter* and this term will be used in this paper) appeared to correlate, although not perfectly fitted, with some of the sintering properties such as the temperatures for shrinkage onset and for maximum shrinkage rate. However, they also pointed out that the most frequent pore diameter can not be truly representative of the entire pore structure. Therefore, one should be interested in realizing which pore parameter other than the overall spectrum of pore-size distribution (it should certainly be the best way of representation of the true green microstructure of interest) within the green powder compacts can be used to perfectly represent the whole pore structure and to reasonably correlate with the sintering behaviour.

0022–2461

Porosity evolution is one of the main phenomena occurring in injection-moulded compacts on debinding. Although it has received great interest [4, 5, 16, 17], only very few have characterized the pore-size distribution (PSD) in the green powder compacts. An efficient particle packing may frequently result in a uniform and narrow PSD, which facilitates densification [18] and leads to the formation of ceramics with desired sintered microstructure.

In a previous study, we have observed that a relatively slow thermolysis favours the formation of green compacts with somewhat narrower PSD than does a faster thermolysis cycle [19]. This encourages the use of lower thermolysis rate under this investigation to explore the influence of solid loading on green microstructure and sintering behaviour of injection-moulded compacts, and will be the focus of this paper. The primary consideration of this investigation is to provide clearer insight upon how the microstructure of the green compacts made by the injection moulding route affects sintering behaviour and what experimentally determined pore parameter can be properly used to provide a reasonable representation of the whole pore structure.

2. Experimental procedures

A low-molecular-weight organic binder composed of paraffin wax (having an average molecular weight 380 and melting point $\sim 60\,^{\circ}C$), vinyl acetate polymer (an average molecular weight of 4500 and melting point $\sim 140\,^{\circ}C$), and stearic acid in varying weight ratio of 6:4:1 were used as major ingredient, minor ingredient, and lubricant, respectively. The wax-based zirconia ceramic suspension with zirconia (HSY3.0, 0.25 μm in average particle size) content of 45–60 vol % was prepared using a ball mill to homogenize the suspension with chloroform as medium. The powder had a fixed volume fraction of 22% relative to the total volume of the powder and the medium for all batches. The organic components can be dissolved entirely into the medium and the resulting powder–binder slurry was dried in air under a vigorously stirring action to ensure suspension homogeneity. The suspension was then granulated through an extruder (Model 70-20vex-6, KCK Industrial Co.), following injection into a cavity of $4 \times 5 \times 60\,mm^3$ dimension with a barrel temperature series of 70–120–140–160–180 °C. The hold pressure was fixed at 90 MPa for 5 s and mould temperature was 45 °C.

The as-moulded compacts were placed into a muffle furnace followed by increasing the temperature to 600 °C for 1 h at a constant heating rate of $5\,^{\circ}C\,h^{-1}$ to completely remove the organic binder. The resulting green compacts after binder removal were characterized using mercury porosimetry (Autopore II 9220). For the mercury porosimetry measurement, a mercury surface tension of $4.85\,N\,cm^{-2}$ and a contact angle of 130° were assumed to calculate the pore size distribution. All measurements were performed under identical procedures for pore size analysis. The sintering behaviour of the powder compacts of $4 \times 4 \times 4\,mm^3$ dimension after binder removal was measured using dilatometry (Netzsch, Model 402E) from room temperature to 1500 °C with a constant heating rate of $5\,^{\circ}C\,min^{-1}$. Microstructure examination of the green compact was performed using scanning electron microscopy (SEM) (Cambridge Instruments, S360).

3. Results and discussion

3.1. Green microstructure

The PSD of the moulded compacts of varying starting solid contents after binder removal is shown in Fig. 1. It is obvious that reducing the solid loading coarsens the resulting pore structure. This observation is reasonable because a larger void space, which is originally the binder phase, is usually expected to develop for a powder–binder blend containing lower solid fraction after binder removal. The PSD for these green compacts is essentially unimodal with fractions of relatively small pores (as represented by the tail-like distribution for each PSD) increasing with increased solid fractions. The most frequent pore diameter decreases from 122 nm, 102 nm, 79 nm to 61 nm, with solids loading increasing from 45, 50, 55 to 60%, respectively. Both the most frequent pore diameter and solid loading correlate well with a correlation factor of 0.986 and this appears to suggest that the most frequent pore diameter can be taken as an indication for the pore structure of the green compacts. This finding, to a certain extent, is in some agreement with observation of previous investigations [10, 20, 21].

The green microstructure of the compacts was examined using the SEM and is shown representatively in Fig. 2 for 50% loading. Generally, the particles are relatively uniform in size distribution and in shape (although they do not have perfectly spherical geometry). The particles are essentially in a random packing configuration with resulting pore size varying from a few nanometres to the order of 300–400 nm. This agrees with the Hg porosimetry-determined PSD shown in Fig. 1. In a closer look at the particle

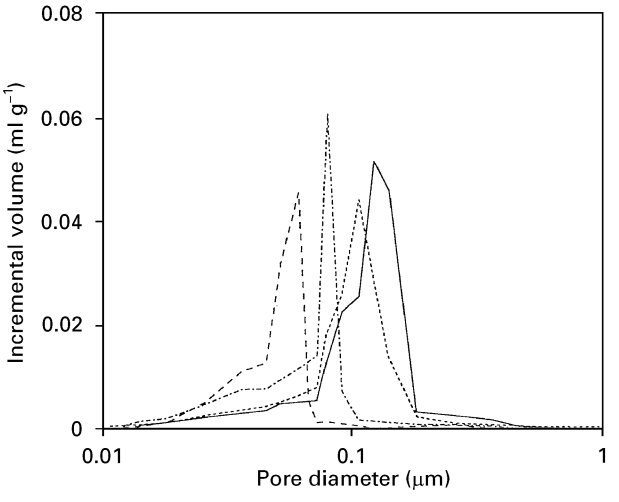

Figure 1 The pore-size distribution of green powder compacts of varying solids loading consolidated by the ceramic injection moulding technique (—) 45%; (- - -) 50%; (-·-) 55%; (— —) 60%.

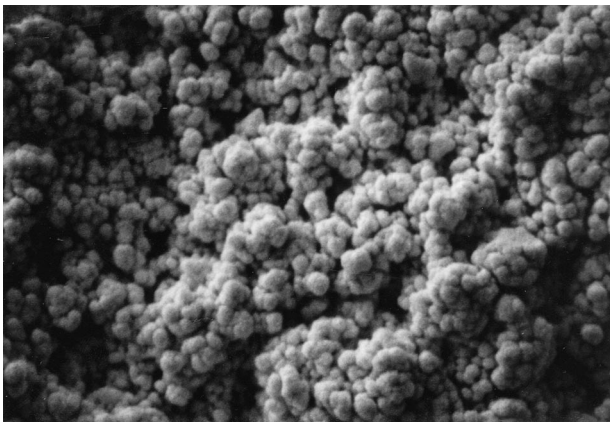

Figure 2 Scanning electron micrograph of the green microstructure of powder compacts with 50% loading.

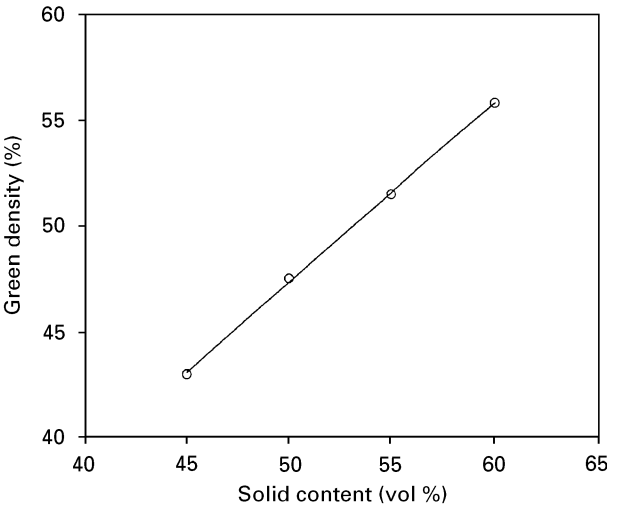

Figure 3 The green density of the green compacts increased linearly with initial solids content.

packing in Fig. 2, a number of particle clusters can be seen (the particles in these clusters are packed densely and the pores within them are relatively small, mostly in the order-of-magnitude of a few nanometres in size). The particle clusters having a size over the range of approximately 1–1.5 μm are considered as agglomerates (no attempt has been made to differentiate between agglomerate and aggregates here) which are supposed to be present in the starting ceramic powder and fail to break into finely divided particles efficiently during the preparation/mixing procedure. These agglomerates could impose considerable effect on microstructure evolution such as coarsening of the green microstructure and altering the sintering behaviour and sintered microstructure [8, 10, 18, 22]. This finding suggests that the ball-mixing following the kneading action currently employed cannot efficiently disperse the powders. A sufficient interparticle attractive force between the fine particles (due to either the van der Waals attraction or to partial interparticle bonding by diffusion) may keep the particles attached and this increases the difficulty in dispersing the powders.

Fig. 3 shows the green density of the compact with respect to the solid content. The green density increases linearly with increasing solids content and is approximately lower by about 2–4 vol % than the expected values. This decrease in effective green density is then verified by a thermogravimetric analysis with which the binder content is measured to be less by approximately 0.6–1 wt % than that at its initially expected content. Such binder loss (corresponding to volume fraction of 2.1–3.5% loss) is believed to take place during the course of kneading and injection moulding because of higher working temperature, i.e. 150–180 °C. Therefore, the resulting porosity is roughly identical to the initial binder content. This finding is obviously different from the experimental results of Shaw and colleagues [23], who observed an increase in effective green density due primarily to the shrinkage of the moulded compact by particle rearrangement during binder removal. However, in the mouldings, the rough similarity in volume fraction between resultant porous phase and initial binder phase suggests little or negligible compact shrinkage occurring on binder removal.

One plausible explanation for this phenomenon may be deduced from the presence of agglomerates (Fig. 2). Agglomeration would frequently significantly reduce particle packing efficiency, resulting in a coarsened PSD and increasing microstructural inhomogeneity. The randomly distributed particles and agglomerates, according to the percolation principle, should be more likely to form an interconnected particulate network (the interconnectivity of the particulate network is expected to be destroyed when the particles are perfectly divided). Such an interconnected network prevents the moulded compact from shrinking to a considerable extent during thermolysis.

Fig. 4 shows a schematic drawing of the compact shrinkage before and after binder removal between two extreme cases. For a perfectly well-dispersed moulded compact, the particles are moved toward a somewhat densely packed feature, causing considerable compact shrinkage (Fig. 4a). However, for a poorly dispersed powder, particles and agglomerates tends to interconnect to form a somewhat rigid network. The continuous particulate network may preserve its original network structure until binder removal (Fig. 4b), even though some of the particles may be free to move during thermolysis. This leads to a negligible compact shrinkage as observed under the current investigation.

3.2. Sintering behaviour

Fig. 5 shows the relative sintered density of the green powder compacts of varying solids loading after sintering at various temperatures. The relative sintered density increased more rapidly for 60% loading than it does for others over the temperature range of 1200–1400 °C. This may be attributed to the fact that the green powder compact of 60% loading possesses a finer PSD characteristic (Fig. 1) than the others and this finer pore structure promotes densification more rapidly. However, the relative sintered densities of these mouldings turn out to be roughly identical, i.e.

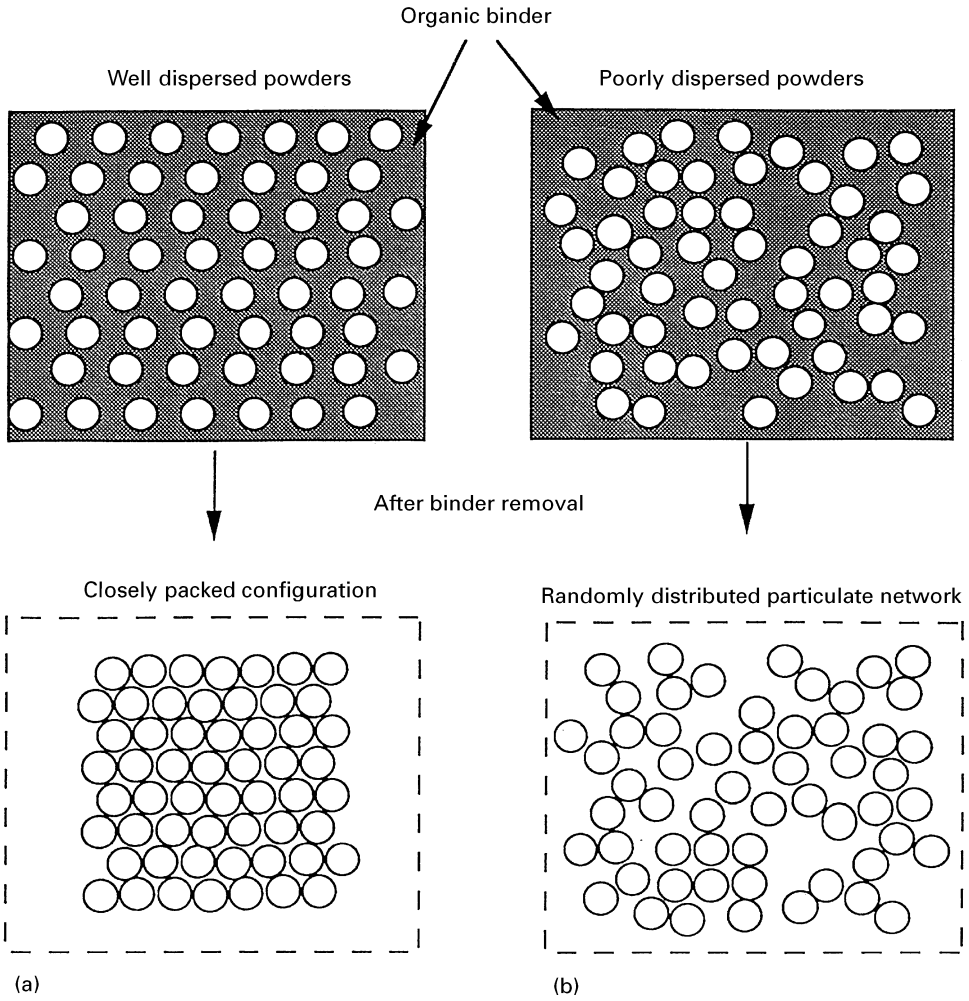

Figure 4 A schematic drawing of particle packing configuration with (a) well-dispersed and (b) poorly dispersed powders, before and after binder removal.

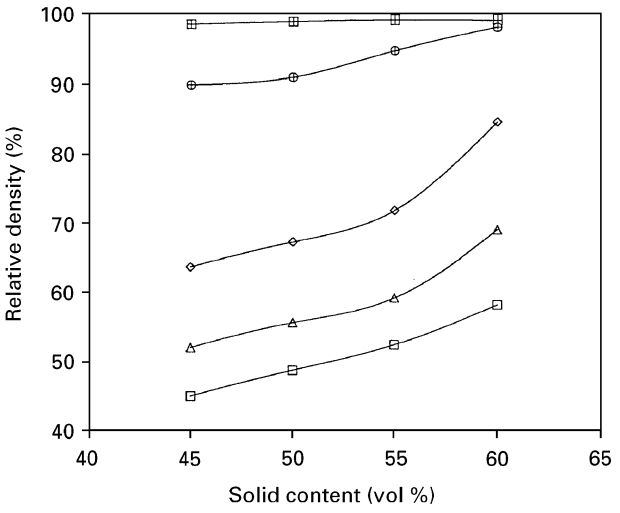

Figure 5 The relative sintered density of the moulded compact of varying solids content at different sintering temperatures, (corresponding to different stages of sintering). (□) 1100 °C; (△) 1200 °C; (◇) 1300 °C; (⊕) 1400 °C; (■) 1500 °C.

about 99% of theoretical, when the temperature reaches 1500 °C. The grain size of the sintered compacts at 1500 °C is approximately 0.4 μm for solids loading below 60% and reaches 0.7 μm for 60% loading, indicating a grain growth effect.

Because densification is a process for pore elimination, it can be deduced from Fig. 5 that a faster rate of pore elimination is observable below ~1300 °C for 60% loading; however, the rate for pore elimination turns to be faster for mouldings with lower solids contents above ~1300 °C. The pore elimination usually accompanies compact shrinkage and it may be reasonable to make a connection that the rate of compact shrinkage can be an indication of the rate for pore elimination. Therefore, it should be possible to provide a more clear demonstration for pore elimination by examining the rate of compact shrinkage and Fig. 6 shows the resulting shrinkage rate curves for varying solids loading. A higher shrinkage rate is seen for 60% powder compact than for others at temperatures below ~1200 °C and over approximately 1260 °C, the compacts with lower solids loading, i.e. 45–55%, exhibit a higher rate of shrinkage. This is consistent with a previous observation in Fig. 5.

Investigations on correlating the PSD with shrinkage phenomena are not extensive [20, 24]. As one realizes, during the course of sintering, the smaller pores tend to be eliminated first (i.e. at lower sintering temperature) and subsequently the larger pores. The higher shrinkage rate at lower temperatures for the 60% compact clearly suggests it be attributed to its finer PSD. Indeed the temperature at which the

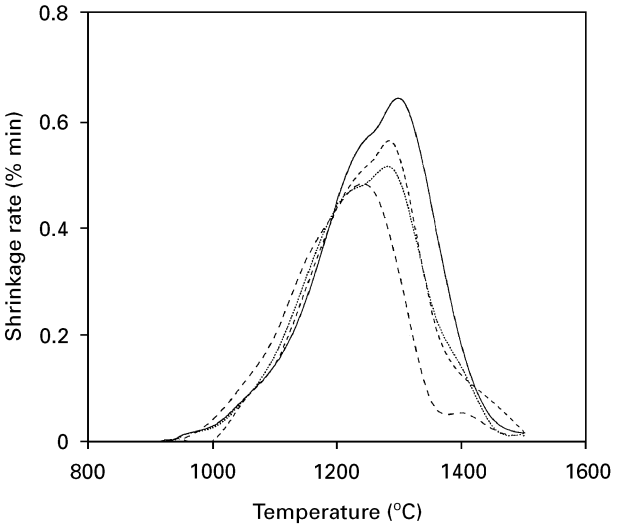

Figure 6 The shrinkage rate of the green compact of varying solids content at various temperatures. (—) 45%; (- - -) 50%; (....) 55%; (– – –) 60%.

maximum shrinkage rate is obtained is lower than the others. Among several researchers, Roosen and Hausner [20] has indicated that the shrinkage-rate curve could be related to the PSD by correlating the maxima in the pore-size frequency distribution (i.e. the most frequent pore diameter) with the maxima of the shrinkage rate curve. By employing their concept, a comparison between Figs 1 and 6 has been made to show a roughly similar shape in their appearance (except that the methods of drawing of these plots are different), which appears to agree with their suggestion.

However, although it does give a somewhat satisfactory result between the green microstructure and corresponding sintering behaviour of a given green powder compact, such comparison may lead to incomplete understanding or a risk of misinterpretation based only on the appearance of their respective curves. This has resulted in a poor correlation between the pore parameter of interest, i.e. the most frequent pore diameter, with respect to a variety of sintering parameters on a series of experiments performed by Roosen and Bowen [10]. Therefore, it may be reasonable to conclude that the most frequent pore diameter is improperly to be given the prime consideration as a true representation of whole pore structure.

Strictly speaking, the most frequent pore diameter represents only a part of the true pore structure. Any spatial inhomogeneity of the PSD because of the presence of inclusions such as agglomerates could alter the sintering (or shrinkage) behaviour to a significant extent [25–28] but causes the most frequent pore diameter little or no change as can be clearly demonstrated by the experiments of Roosen and Bowen [10]. Therefore, it should be necessarily important to take any possible microstructural change due to incorporation of inhomogeneity into consideration and we expect that such a pore parameter should be strongly related to the presence of microstructural inhomogeneities.

By examining a number of porosimetry-determined pore parameters, the average pore diameter has been observed to be strongly sensitive to the variation of microstructure. The average pore diameter is determined by dividing the volume-averaged pore diameter with respect to the surface area-averaged pore diameter in the calculation of intrusion data on mercury porosimetry. Any variation in local microstructural inhomogeneity leads to a change in these average pore parameters and thus causes a variation in the resulting average pore diameter. Therefore, we ascertained that the average pore diameter itself contains more information on the true pore structure than does the most-frequent pore diameter for a given powder compact.

Plotting the relative sintered density versus the average pore diameter results in fairly good correlation as depicted in Fig. 7, with correlation coefficients in the range of 0.976–0.995 for all temperatures, which is much better correlation than for the most frequent pore diameter, i.e. having coefficients of 0.894–0.953. The sintered density is linearly, inversely proportional to the average pore diameter and this relationship is consistent with a previous observation on the sintering of injection-moulded alumina powder compacts [29]. Such a linearity between different sintering temperatures and average pore diameter suggests that the average pore diameter could be capable of representing the whole pore structure and can be reasonably used to characterize the sintered microstructure during different stages of sintering.

The temperature at which the maximum shrinkage rate is attained is generally considered as the stage for elimination of small intra-agglomerate pores or of the most-frequent pores in the pore-size distribution. The smaller the pore size, the lower the temperature at maximum shrinkage rate that can be achieved. Therefore, a correlation between the temperature and the most frequent pore diameter should accordingly exhibit a satisfactory result and a correlation factor of 0.939 is obtained which appears to agree with the above argument. However, an attempt to correlate the

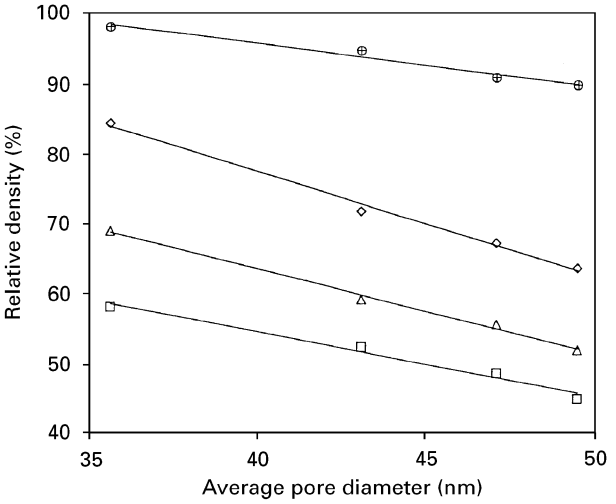

Figure 7 Linear correlation between relative sintered density and average pore diameter at various sintering temperatures. (□) 1100 °C; (△) 1200 °C; (◇) 1300 °C; (⊕) 1400 °C.

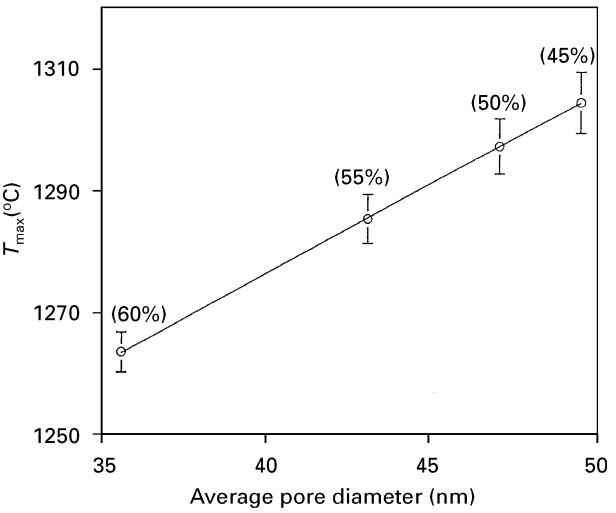

Figure 8 The temperature of maximum shrinkage rate increased linearly with increasing average pore diameter.

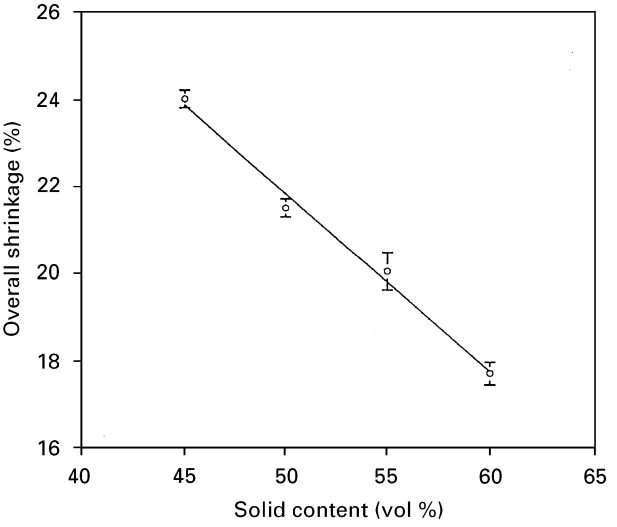

Figure 9 The overall shrinkage of the green compacts at various body orientations (expressed by the standard deviation bars) for green compact of varying solids loading showing negligible orientation-dependent shrinkage which is indicative of an isotropic shrinkage characteristic.

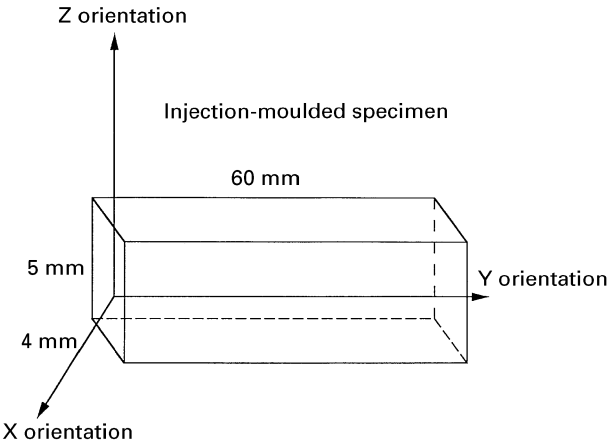

Figure 10 A schematic drawing of the injection-moulded compact with the definition of three axial orientations.

temperature (denoted as T_{max}) with respect to the average pore diameter is made as shown in Fig. 8 which surprisingly yields a perfectly fitted linear relation, i.e. correlation coefficient of 1.000 (the error bars in Fig. 8 represent the standard deviation of three measurements for each solids content). This further suggests that the average pore structure is practically applicable as a satisfactory indicator to correlate with both the green microstructure and corresponding sintering behaviour.

Although the relationship of Fig. 8 provides some evident clues on realizing how T_{max} changes with the pore structure, one may ask what T_{max} stands for during the course of sintering. If only the shape similarity between the pore-size distribution and the shrinkage-rate curves is considered as suggested by Roosen and Hausner [20], then T_{max} is reasonably considered to be the temperature at which the most frequent pores are eliminated. The larger the most-frequent pores, the higher the T_{max} that results. Unfortunately, the poorer correlation of T_{max} with the most frequent pore diameter than with the average pore diameter suggests that some additional factors, such as agglomerates, other than the most-frequent pores control T_{max}. That is to say the T_{max} cannot be purely represented by the most-frequent pore structure. Instead, it can be best described by means of the average pore structure, i.e. a combination of both the volume-based and surface area-based average pore structure.

3.3. Shrinkage isotropy

Numerous investigations have focused on the shrinkage phenomenon of a bulk green compact during high-temperature sintering and have observed, in most cases, shrinkage anisotropy, which is a complex function of powder morphology (e.g. agglomerates), degree of microstructural inhomogeneity, and methods of consolidation [22, 25, 30, 31]. However, little publication on the orientation-dependent shrinkage behaviour of injection-moulded powder compacts has been reported in literature. From the dilatometric analysis, the overall shrinkage of the compacts with varying orientations is shown in Fig. 9 for different solids contents. The error bars represent the standard deviation of the shrinkage of varying orientations, which falls in the range of 0.2–0.4% for all solids loading. Such a relatively small variation in shrinkage for different compact orientations suggests that the shrinkage of the injection-moulded compacts during high-temperature sintering is essentially isotropic, even under a high moulding pressure of 90 MPa. Such a unique characteristic can only be observed for powder compacts having physically (and chemically) homogeneous microstructure. The presence of agglomerates as previous discussed is expected to have some influence on shrinkage and the error bars in Fig. 9 may be a gross effect of the agglomerates. A further analysis by examining the shrinkage-rate curves for moulded compacts of 55% loading for three principal orientations (as depicted in Fig. 10 for X, Y, and Z orientations) is illustrated in Fig. 11. The shape and peak location of these curves are roughly similar for

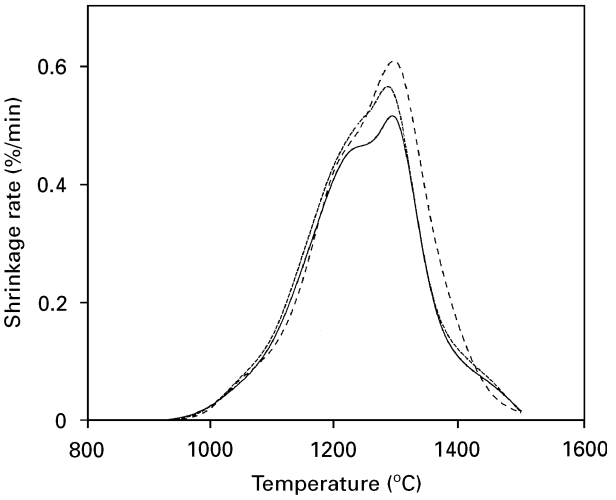

Figure 11 The shrinkage rate of green compact (55% loading) at different orientations (—) X; (– – –) Y; (- - - -) Z.

the same compacts except for some difference in shrinkage rate. Such a slight difference in shrinkage rate, although a lack of direct evidence, is supposed to be attributed to a certain inhomogeneous distribution of the agglomerates. In fact, the microstructural difference of the green compact can hardly be distinguished from each orientation from microscopy examination. On the basis of the present understanding, one may conclude that, although local inhomogeneities present, the injection-moulded compacts presently developed possess a significant degree of physically homogeneous microstructure throughout the injection-moulded body.

4. Conclusion

The influence of solid loading of injection-moulded compacts on the green microstructure and sintering behaviour is investigated. The presence of agglomerates (i.e. poorly-dispersed powders) causes the formation of interconnected particulate network and this unique structure retains the moulded compact free from volume change (i.e. shrinkage) after removing the binder. In spite of the presence of agglomerates, the moulded compacts illustrate a significant degree of homogeneity as revealed by their orientation-independent uniformity in shrinkage phenomenon on sintering and it may be reflected as a result of the achievement of near-perfectly random distribution of the agglomerates throughout the moulded compacts. The average pore diameter appears to offer more reliable correlation between the green microstructure and corresponding sintering behaviour than does the most frequent pore diameter which represents only a part of the whole pore structure. The remarkably excellent correlation between the average pore diameter and sintering properties suggests that the average pore structure is capable of representing the whole pore structure of a given powder compact.

Acknowledgements

The authors are gratefully indebted to the Ministry of Economic Affairs, Taiwan for funding and supporting this research under contract No. 863KG2230.

References

1. J. J. BURKE, E. N. LENOE and R. N. KATZ (eds), "Ceramics for high performance applications II" (Brook Hill Publishing Co., Chestnut Hill, MA, 1978).
2. R. M. GERMAN, "Powder injection molding" (Metal Powder Industries Federation, Princeton, NJ, 1990).
3. B. C. MUTSUDDY and R. G. FORD, "Ceramic injection molding" (Chapman & Hall, London, 1995).
4. H. M. SHAW and M. J. EDIRISINGHE, *J. Eur. Ceram. Soc.* **13** (1994) 135.
5. S. A. MATAR, M. J. EDIRISINGHE, J. R. G. EVANS and E. H. TWIZELL, *J. Mater. Res.* **8** (1993) 617.
6. M. J. CIMA, J. A. LEWIS and A. D. DEVOE, *J. Amer. Ceram. Soc.* **72** (1989) 1192.
7. E. A. BARRINGER and H. K. BOWEN, *ibid.* **62** (1982) c199.
8. W. H. RHODES, *ibid.* **64** (1981) 19.
9. F. DOGAN, A. ROOSEN and H. HAUSNER, *Sci. Ceram.* **13** (1985) 231.
10. A. ROOSEN and H. K. BOWEN, *J. Amer. Ceram. Soc.* **71** (1988) 970.
11. D. M. LIU and W. J. TSENG, *Ceram. Int.* in press.
12. M. SAKARCAN, C. H. HSUEH and A. G. EVANS, *J. Amer. Ceram. Soc.* **66** (1983) 456.
13. T. IKEGAMI and Y. MORIYOSHI, *ibid.* **67** (1984) 174.
14. M. A. C. G. VAN DE GRAAF, K. KEIZER and A. J. BURGGRAAF, *Sci. Ceram.* **10** (1979) 83.
15. P. H. RIETH, J. S. REED and A. W. NAUMANN, *Amer. Ceram. Soc. Bull.* **55** (1976) 717.
16. H. M. SHAW, T. J. HUTTON and M. J. EDIRISINGHE, *J. Mater. Sci. Lett.* **11** (1993) 1075.
17. P. CALVERT and M. CIMA, *J. Amer. Ceram. Soc.* **72** (1989) 575.
18. T. S. YEH and M. D. SACKS, *J. Amer. Ceram. Soc.* **71** (1988) 484.
19. D. M. LIU and W. J. TSENG, *Acta. Mater.* (in review).
20. A. ROOSEN and H. HAUSNER, *Adv. Ceram.* **12** (1984) 714.
21. R. PAMPUCH and K. HABERKO, in "Ceramic powders", edited by P. Vincenzini, (Elsevier, Amsterdam, 1983) p. 623.
22. E. LINIGER and R. RAJ, *J. Amer. Ceram. Soc.* **70** (1987) 843.
23. H. M. SHAW and M. J. EDIRISINGHE, *J. Eur. Ceram. Soc.* **15** (1995) 109.
24. T. J. CARBONE and J. S. REED, *Amer. Ceram. Soc. Bull.* **57** (1978) 748.
25. K. D. REEVE, *Amer. Ceram. Soc. Bull.* **42** (1963) 452.
26. M. D. SACKS and J. A. PUSK, *J. Amer. Ceram. Soc.* **65** (1982) 70.
27. F. F. LANGE, *ibid.* **67** (1984) 83.
28. J. ZHAO and M. P. HARMER, *ibid.* **71** (1988) 113.
29. D. M. LIU, *Ceram. Int.* in press.
30. A. G. EVANS, *J. Amer. Ceram. Soc.* **65** (1982) 497.
31. TSUNG-HSING LEU, MS Thesis, National Cheng Kong University, Tainan, Taiwan, 1992.

Received 28 August 1996
and accepted 17 June 1997